

Electronic Supplementary Information

Interface Engineering for a Rational Design of Poison-free Bimetallic CO Oxidation Catalysts

Kihyun Shin^{1,†}, Liang Zhang^{2,†,‡}, Hyesung An³, Hyunwoo Ha³, Mi Yoo³, Hyuck Mo Lee¹,
Graeme Henkelman², and Hyun You Kim^{3,*}

¹Department of Materials Science and Engineering,
KAIST, 291-Daehak-ro, Yuseong-gu, Daejeon, 34141 Korea

²Department of Chemistry and the Institute for Computational Engineering and Sciences,
University of Texas at Austin, Austin TX USA

³Department of Materials Science and Engineering,
Chungnam National University, 99-Daehak-ro, Yuseong-gu, Daejeon, 34134 Korea

Microkinetic modelling

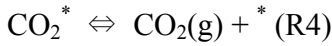
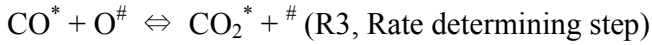
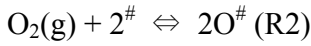
Fig. S1~S11

XYZ coordinates of selected structure models

Micro kinetic model for bifunctional CO oxidation by Pt@Cu_FNP

CO oxidation by Pt-CO* and Cu-2O*

The micro-kinetic model¹ for bifunctional CO oxidation by Pt-CO* and Cu(100)-O* or Cu(111)-O* of Pt@Cu_FNP, the results of which are presented in Fig. 3a~c is as follows:



Here, the rate of CO₂ formation is equal to the maximum rate of the reaction R3. Because the first two reactions are in equilibrium, the rate of these reactions can be written as:

$$\text{rate(R1)} = k_1^+ p(\text{CO})\theta_* - k_1^- \theta_{\text{CO}} \rightarrow \theta_{\text{CO}} = \left(\frac{k_1^+}{k_1^-} \right) p(\text{CO})\theta_* = K_1 P(\text{CO})\theta_*$$

$$\text{rate(R2)} = k_2^+ p(\text{O}_2)\theta_\#^2 - k_2^- \theta_{\text{O}}^2 \rightarrow \theta_{\text{O}} = \sqrt{\left(\frac{k_2^+}{k_2^-} \right) p(\text{O}_2)\theta_\#} = \sqrt{K_2 P(\text{O}_2)}\theta_\#$$

The maximum rate of R3 is:

$$\text{rate(R3)}^{\text{max}} = k_3^+ \theta_{\text{CO}}\theta_{\text{O}} = k_3^+ K_1 p(\text{CO})\sqrt{K_2 P(\text{O}_2)}\theta_*\theta_\#$$

where K₁ and K₂ are the equilibrium constants for R1 and R2, p(CO) and p(O₂) are the partial pressures of CO and O₂. k_i⁺ and k_i⁻ are the forward and the backward rate constant for R_i, respectively.

The overall rate of CO₂ formation, $\text{rate}(R3)^{\text{max}}$ is:

$$\text{rate}(R3)^{\text{max}} = k_3^+ \theta_{CO} \theta_O$$

The reaction R1 and R2 concerns the adsorption of CO and O₂, respectively. Therefore, the equilibrium constants K1 and K2 are,

$$K1 = \exp\left(\frac{-\Delta G1}{kT}\right) = \exp\left(\frac{-(\Delta E1 - T\Delta S1 + \Delta ZPE)}{kT}\right)$$

$\Delta E1$: Energy of CO adsorption

$\Delta S1$: Entropy change involved in CO adsorption

ΔZPE : Zero point energy change upon CO adsorption = -0.07 eV

and

$$K2 = \exp\left(\frac{-\Delta G2}{kT}\right) = \exp\left(\frac{-(\Delta E2 - T\Delta S2 + \Delta ZPE)}{kT}\right)$$

$\Delta E2$: Energy of O₂ adsorption

$\Delta S2$: Entropy change involved in O₂ adsorption

ΔZPE : Zero point energy change upon O₂ adsorption = -0.05 eV

The sum of the coverage of adsorbed O, CO and free adsorption sites is equal to 1, so that:

$$\theta_{CO} + \theta_O + \theta_* + \theta_{\#} = 1$$

where θ_{CO} , θ_O , θ_* , and $\theta_{\#}$ are the coverage of adsorbed CO, adsorbed O, and free sites of the surface for CO (*) and O (#) adsorption.

Because the bifunctional CO oxidation pathways described in Fig. 3a, and b utilizes CO molecules adsorbed on the Pt-edge sites, we regarded the Pt-edge sites as an available CO binding site. For oxygen supplied by Cu(100) or Cu(111), the total number of Cu(100) or Cu(111) atoms were counted and estimated as an active O binding site.

For the reaction at the Pt-Cu(100) interface, the surface fraction of Cu(100) sites (54/102) and Pt edge sites (48/102) of Pt@Cu_F NP was as follows:

$$\theta_{CO} + \theta_* = \frac{48}{102} = 0.471, \quad \theta_O + \theta_{\#} = \frac{54}{102} = 0.529.$$

The maximum value of θ_{CO} and θ_O can be set to 0.471 and 0.529, respectively.

For the reaction at the Pt-Cu(111) interface, the surface fraction of Cu(111) sites (48/96) and Pt edge sites (48/96) of Pt@Cu_F NP was as follows:

$$\theta_{CO} + \theta_* = \frac{48}{96} = 0.50, \quad \theta_O + \theta_{\#} = \frac{48}{96} = 0.50,$$

The maximum value of θ_{CO} and θ_O can be set to 0.50.

We found that even at 600K, calculated θ_{CO} and θ_O values are not significantly differing from the values estimated from the site fraction.

Note that we hypothesized that, despite the noticeable level of E_{des} of CO₂ was found, the surface concentration of CO₂ like intermediate (S3 in Fig. 3a, and b), CO₂^{*} in R4, is marginally small because the partial pressure of the product (p(CO₂)) is low and the prefactor of desorption is generally at least one order or more greater than that of adsorption.¹

For R3, the maximum rate can be obtained as follows:

$$rate(R3)^{max} = k_3^+ \theta_{CO}^{max} \theta_O^{max}$$

where,

$$k_3^+ = \frac{kT}{h} \exp\left(\frac{-\Delta G_3^+}{kT}\right) = \frac{kT}{h} \exp\left(\frac{-(E_{act} - T\Delta S_3^+)}{kT}\right)$$

E_{act} : Activation energy for reaction 3

$$\Delta S_3^+ = 0$$

rate(R3)^{max} was calculated at p(CO)=0.01 bar and p(O₂)=0.21 bar. Temperature dependent standard entropy of CO and O₂ was considered and adopted from NIST webbook (<http://webbook.nist.gov>).

Fig. S1

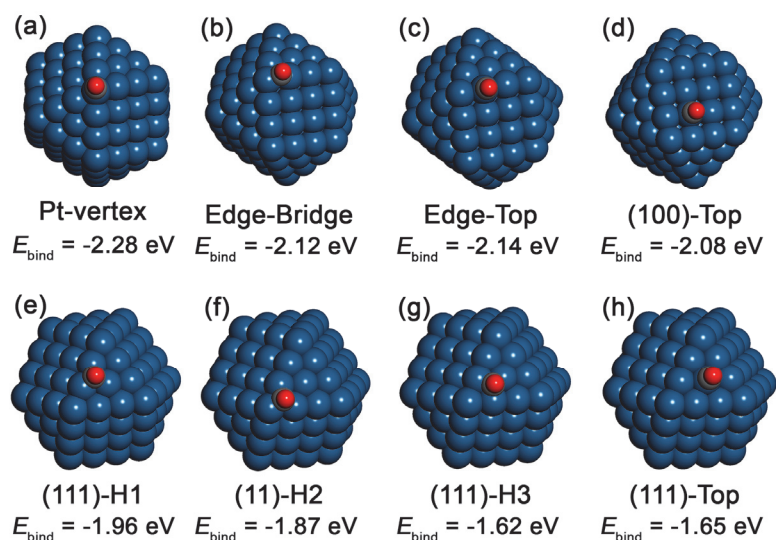


Fig. S1. Optimized adsorption geometry of CO on Pt₁₄₇ NP and corresponding binding energy, E_{bind} .

Fig. S2

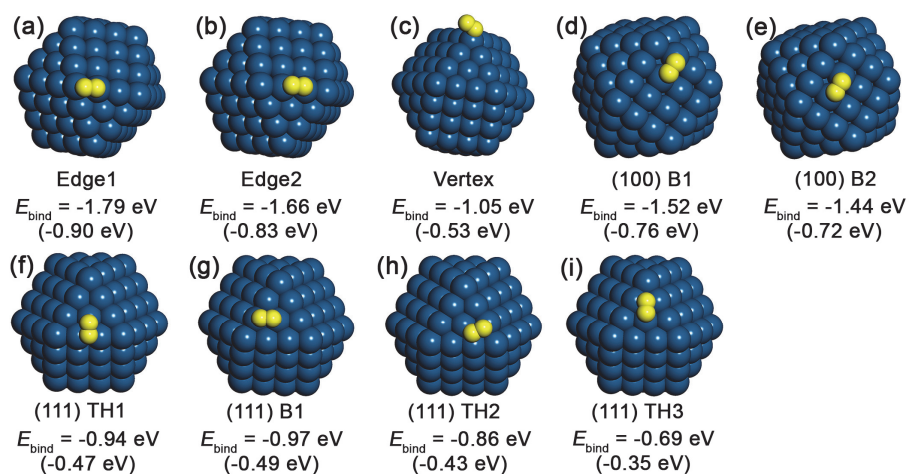


Fig. S2. Optimized molecular adsorption geometry of O₂ on Pt₁₄₇ NP and corresponding binding energy, E_{bind} . Values in the parentheses present the E_{bind} per single binding site.

Fig. S3

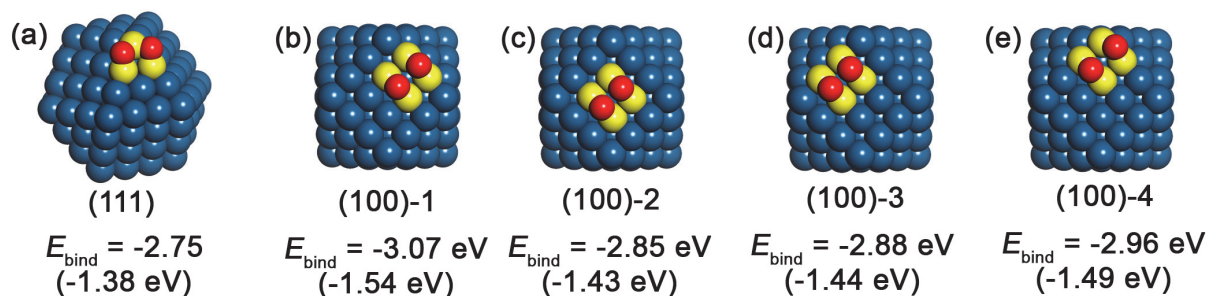


Fig. S3. Optimized dissociative adsorption geometry of O_2 on Pt_{147} NP and corresponding binding energy, E_{bind} . Values in the parentheses present the E_{bind} per single binding site.

Fig. S4

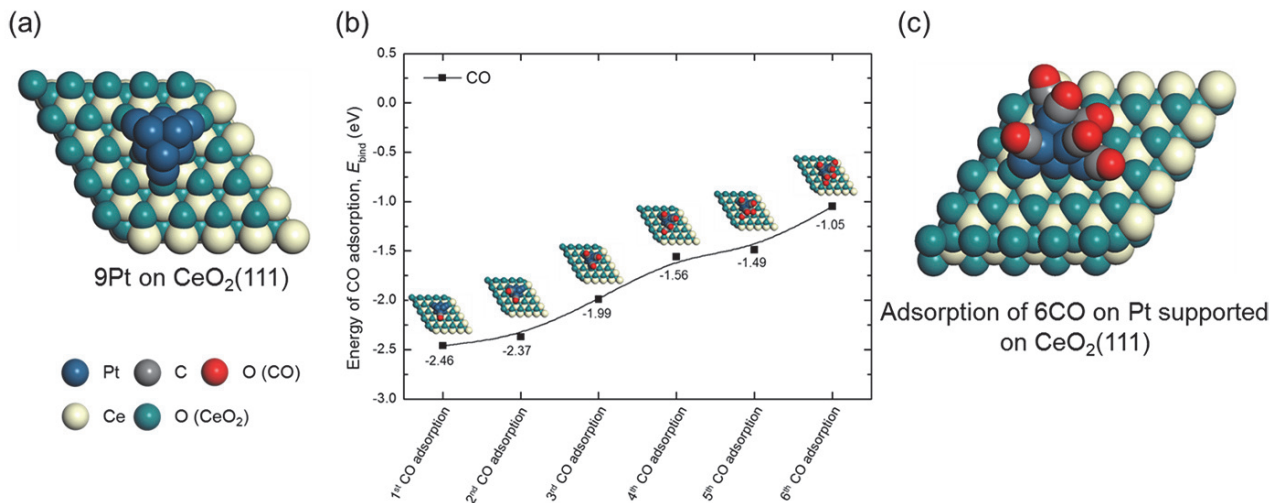


Fig. S4. Coverage dependent E_{bind} of CO molecules on $\text{CeO}_2(111)$ supported Pt_9 NP. (a) The initial geometry of Pt_9/CeO_2 , (b) The E_{bind} presented as a function of CO coverage, and (c) Pt_9/CeO_2 with 6 CO molecules. We found that Pt_9 cannot stably bind more than 6 CO molecules. The open Pt sites at the Pt- CeO_2 perimeter could not bind CO molecules. Rather, the NP was disordered.

Fig. S5

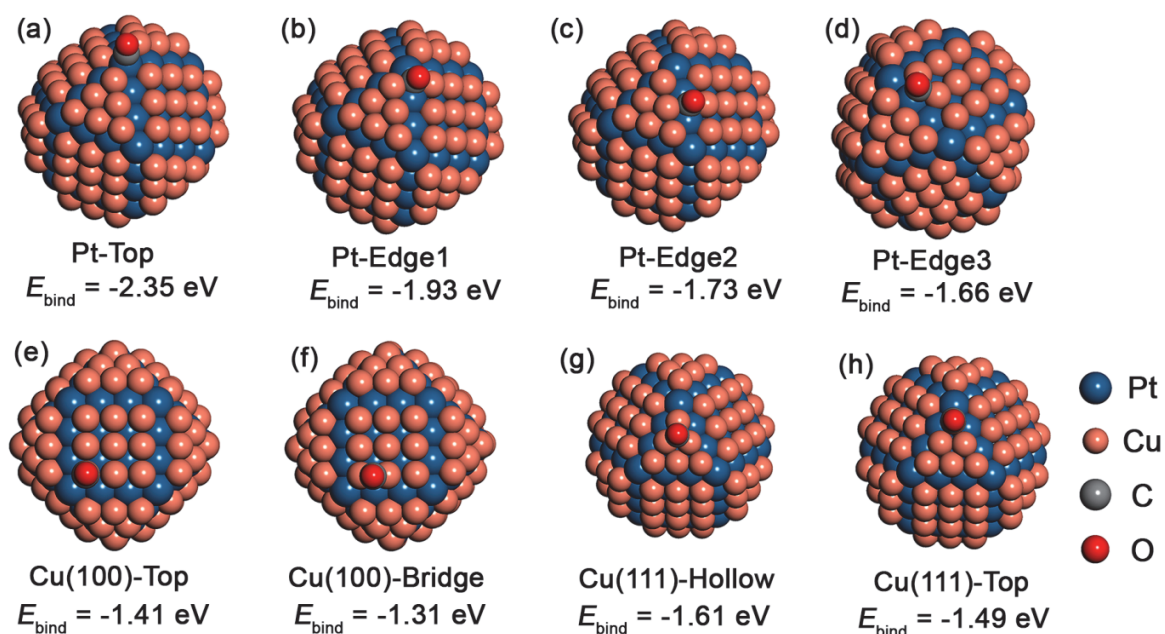


Fig. S5. Optimized adsorption geometry of CO on Pt@Cu_F NP and corresponding binding energy, E_{bind} .

Fig. S6

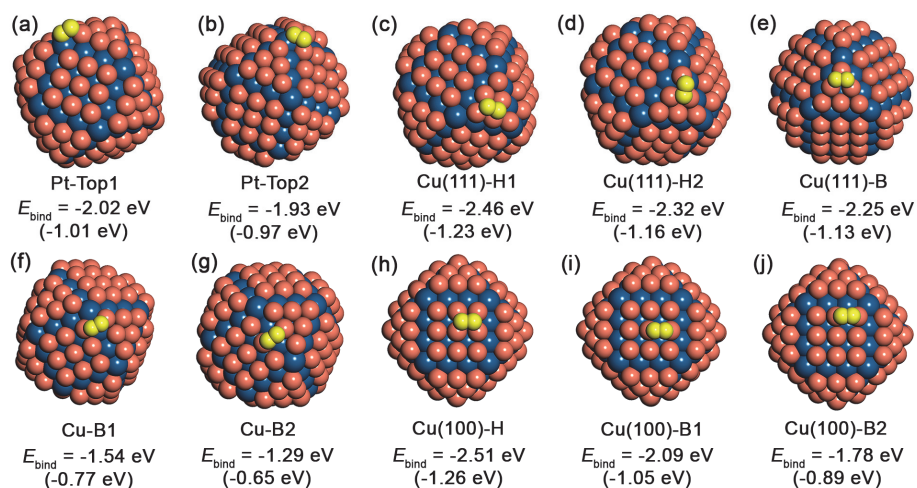


Fig. S6. Optimized adsorption geometry of O₂ on Pt@Cu_F NP and corresponding binding energy, E_{bind} .

Values in the parentheses present the E_{bind} per single binding site.

Fig. S7

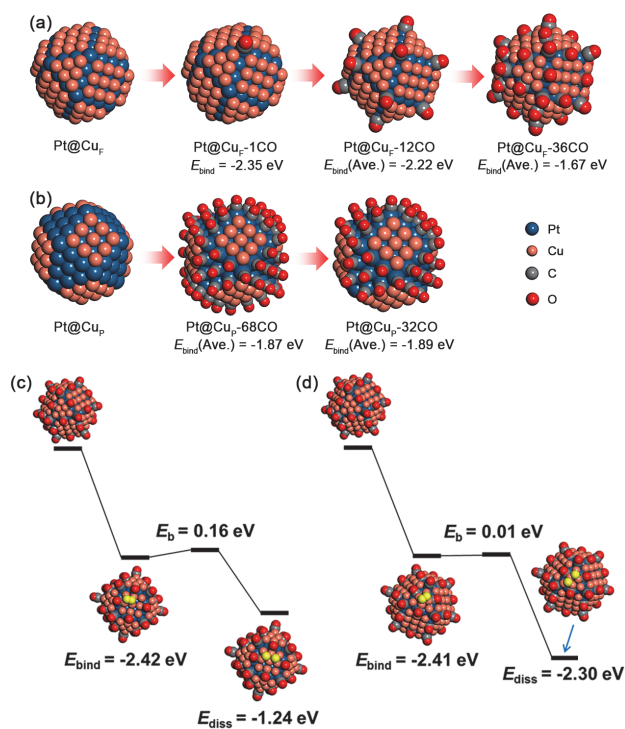


Fig. S7. CO saturated NPs for CO oxidation calculations: (a) Pt@Cu_F, (b) Pt@Cu_P. Because Pt preferentially binds CO all available Pt sites were covered with CO. The last image of (b) presents the half-NP model. (c) and (d) presents the dissociation of molecularly bound O₂ on Cu(100) and Cu(111) in the presence of pre-adsorbed CO molecules. Yellow spheres in (c) and (d) denotes oxygen atoms.

Fig. S8

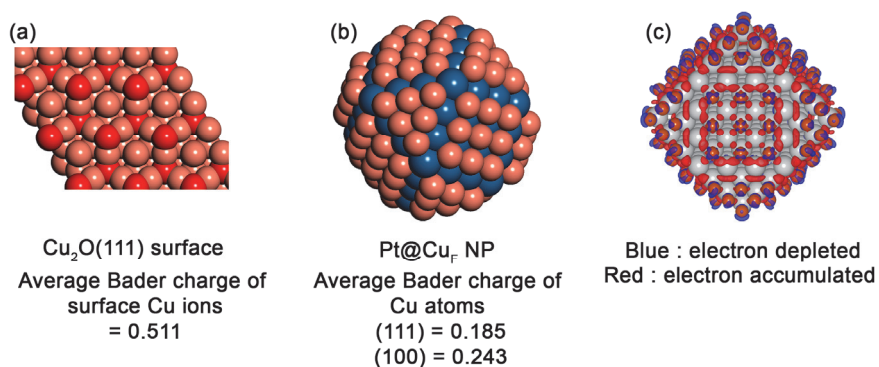


Fig. S8. Electronic analysis of $\text{Cu}_2\text{O}(111)$ surface and Pt@Cu NP. (a) Bader charge analysis of $\text{Cu}_2\text{O}(111)$ surface. Red spheres represent oxygen atoms. (b) Bader charge analysis of Pt@Cu_F NP. Cu atoms are reduced. (c) Electron density difference map upon Cu deposition on Pt_{147} NP. Cu donates electron density to Pt. Blue and red area represents the electron depleted or accumulated orbitals, respectively. Grey and dark orange spheres represent Pt and Cu.

Fig. S9

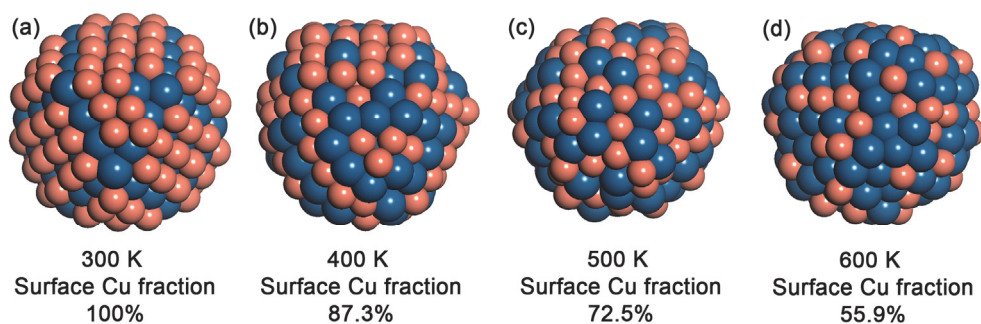


Fig. S9. Snapshots of Pt@Cu_F NPs after 300 ns of MD simulation at corresponding temperature. (a) 300 K, (b) 400 K, (c) 500 K, and (d) 600 K. Numbers below show the fraction of the remaining surface Cu atoms after 300 ns of MD simulation.

Fig. S10

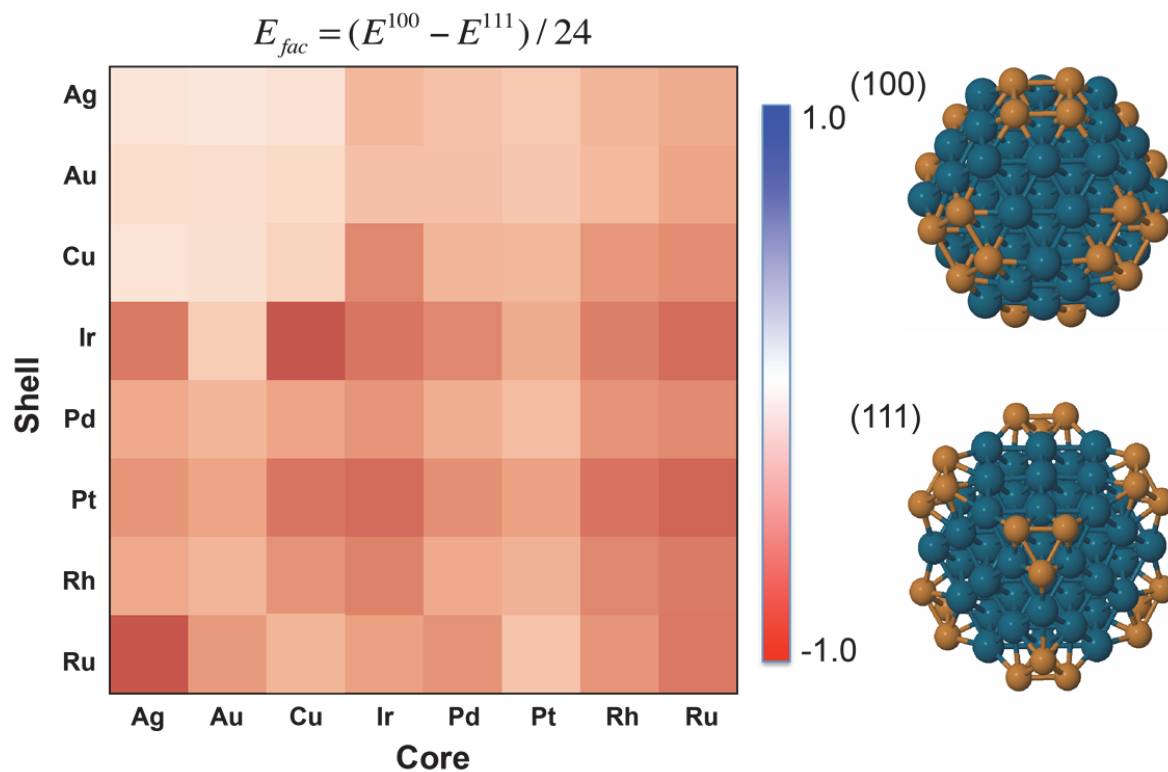


Fig. S10. E_{fac} over tested 56 X@Y core@shell NPs. Negative (red) E_{fac} indicates (100) shells are more stable than (111) shells. Positive (blue) E_{pref} denotes the reverse case. E^{100} and E^{111} are the total energy of X@Y NPs with geometries showing on the right side, respectively. All the X@Y NPs prefer to occupy (100) facets first.

Fig. S11

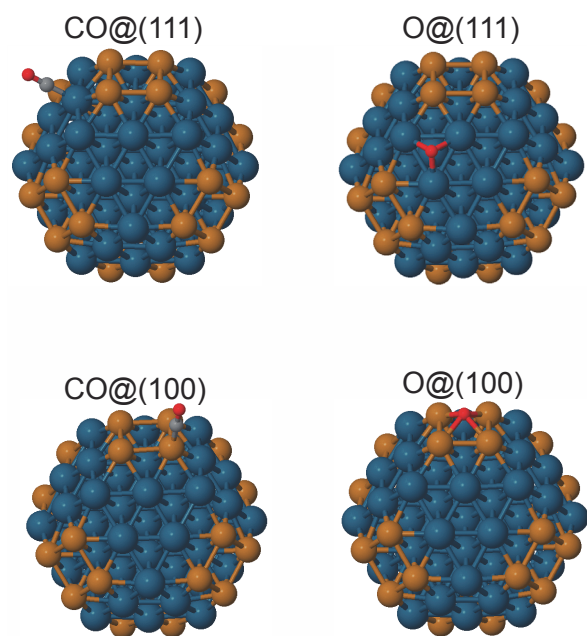


Fig. S11. Binding geometries of O and CO at (111) and (100) facets on $X@Y_p$ NPs

References

- 1 I. Chorkendorf and J. W. Niemantsverdriet, *Concepts of Modern Catalysis and Kinetics*; Wiley-VCH: Weinheim, 2007.

Cu	0.0709680	12.3853910	15.8231930	O	3.3295760	20.2637060	14.1276990
Cu	15.7276880	4.9555660	10.6065650	O	20.8251200	10.1682260	14.2384580
Cu	16.9452820	7.0691040	10.5918110	O	-3.2320881	10.0357000	14.2327620
Cu	15.6452520	6.3982260	8.4436810	O	17.8761000	10.9979210	19.2954970
Cu	15.6577040	3.4176700	12.7027870	O	0.4508270	10.9677950	19.2983700
Cu	16.9497950	5.6739120	12.5901200	O	0.4462610	9.3053550	9.2032760
Cu	18.2468040	7.9339300	12.6732330	O	17.8730770	9.3316450	9.1986750
Cu	2.6075580	4.9319470	10.6112890	O	4.1102370	2.9792890	9.2433440
Cu	1.3867630	5.6453900	12.5967010	O	5.4814580	12.2124050	5.0632450
Cu	2.6857300	3.3945890	12.7113240	O	12.9075140	17.9108730	9.1105660
Cu	2.6823290	6.3746610	8.4475160	O	14.2048790	17.3295590	19.2610670
Cu	1.3830680	7.0419990	10.5960330	O	12.8228890	8.0944660	23.4408710
Cu	0.0841460	7.8932930	12.6761790	O	5.5148500	2.2307250	19.3467520
Cu	7.9510670	1.8988330	17.9681140	O	5.5158240	8.0907930	23.4463600
Cu	9.1710870	1.1866100	15.9820280	O	12.8130570	12.2144330	5.0529880
Cu	6.5622260	1.1779910	15.8794750	O	5.4152300	17.9153440	9.1763780
Cu	9.1719670	2.7004410	20.1204190	O	14.2336860	2.9975810	9.2421090
Cu	10.3923570	1.8995100	17.9680140	O	12.8268840	2.2302380	19.3418910
Cu	11.7757450	1.1828030	15.8815760	O	4.1011750	17.3158220	19.2729940
Cu	9.1591240	19.2225670	12.6099510	O	17.8850600	5.1414240	15.1896310
Cu	10.4659470	18.4539430	10.4663860	O	0.4343480	15.1696690	13.2921810
Cu	11.7645870	19.1574720	12.6152410	O	9.1239200	20.1188080	15.3129110
Cu	6.3049810	19.1791640	12.8259250	O	0.4505780	5.1248850	15.2085860
Cu	7.8246930	18.5961960	10.4099040	O	9.1735210	0.0959750	13.3852830
Cu	9.1984420	17.4841440	8.0919050	O	17.8759270	15.1918850	13.3025520
Cu	16.9394200	14.6610510	15.9091570	O	9.1624920	5.8761410	5.1009370
Cu	15.7153340	15.3749470	17.8987580	O	9.1584820	14.4216760	23.4086280
Cu	15.6388570	16.9074580	15.8031800	O	9.2542870	19.0169590	9.1182720
Cu	18.2434120	12.4146550	15.8211330	O	7.6156940	19.9779920	11.8011460
Cu	16.9397100	13.2639470	17.9100240				
Cu	15.6376670	13.9353110	20.0618870				
C	3.9113830	13.2085540	22.7542740				
C	14.3963890	7.1020500	5.7353970				
C	14.4208800	19.2085300	14.1830180				
C	3.9183540	1.1089510	14.3136670				
C	9.1371730	16.2040150	5.7060100				
C	9.1698740	4.1567880	22.8175860				
C	14.3801190	13.2048720	22.7787330				
C	3.9376240	7.0835360	5.7294770				
C	14.4081110	1.1180320	14.3088730				
C	3.9482710	19.2287080	14.1559650				
C	19.6192430	10.1689090	14.2410250				
C	-2.0264201	10.0540760	14.2394650				
C	16.8590220	11.2152200	18.5935110				
C	1.4628040	11.1967280	18.5927960				
C	1.4654560	9.1001080	9.9048240				
C	16.8549020	9.1224360	9.9010100				
C	4.4253440	3.9740250	9.9394360				
C	6.1887730	11.8158990	6.0202040				
C	12.1161510	17.2694350	9.8486440				
C	13.8922870	16.3340540	18.5645680				
C	12.1270040	8.4939460	22.4765500				
C	6.2116040	2.9986100	18.6405310				
C	6.2087980	8.4882920	22.4792620				
C	12.1090970	11.8162390	6.0118400				
C	6.2568130	17.3215690	9.9038570				
C	13.9068420	3.9899000	9.9362970				
C	12.1319940	3.0032690	18.6397910				
C	4.4113900	16.3223900	18.5728590				
C	16.8669930	5.7306390	14.7535440				
C	1.4502690	14.5874620	13.7414360				
C	9.1386670	19.0102400	14.7168570				
C	1.4657010	5.7079580	14.7582420				
C	9.1700500	1.2725430	13.8203470				
C	16.8578580	14.6060130	13.7420230				
C	9.1603810	6.6923380	6.0535920				
C	9.1593330	13.6176540	22.4455550				
O	3.2893180	13.5537040	23.7278560				
O	15.0067220	6.7517740	4.7561230				
O	15.0366770	20.2448930	14.1574740				
O	3.2983470	0.0749510	14.3293690				
O	9.1176360	16.8980190	4.7197400				
O	9.1703810	3.4625010	23.8036320				
O	14.9793670	13.5435420	23.7688400				
O	3.3358480	6.7268280	4.7472890				
O	15.0221630	0.0803650	14.3222490				